2018

Climate Change and Mountaintop Removal Mining: A MaxEnt Assessment of the Potential Dual Threat to West Virginia Fishes

Lindsey R F Hendrick
Virginia Commonwealth

CLIMATE CHANGE AND MOUNTAINTOP REMOVAL MINING: A MAXENT ASSESSMENT OF THE POTENTIAL DUAL THREAT TO WEST VIRGINIA FISHES

A thesis submitted in partial fulfillment of the requirements for the degree of Master of Science at Virginia Commonwealth University.

by

Lindsey R. F. Hendrick

Master of Science, Virginia Commonwealth University 2018

Bachelor of Science, Hollins University 2016

Director: Daniel J. McGarvey, Ph.D.

Associate Professor

Center for Environmental Studies

Virginia Commonwealth University

Richmond, Virginia

April 2018

Table of Contents

List of Tables and Figures

Abstract

CLIMATE CHANGE AND MOUNTAINTOP REMOVAL MINING: A MAXENT ASSESSMENT OF THE POTENTIAL DUAL THREAT TO WEST VIRGINIA FISHES

By Lindsey R. F. Hendrick, Bachelor of Science

A thesis submitted in partial fulfillment of the requirements for the degree of Master of Science at Virginia Commonwealth University.

Virginia Commonwealth University, 2018

Major Director: Daniel J. McGarvey, Ph.D., Center for Environmental Studies

Accounts of species' range shifts in response to climate change, most often as latitudinal shifts towards the poles or upslope shifts to higher elevations, are rapidly accumulating. These range shifts are often attributed to species 'tracking' their thermal niches as temperatures in their native ranges increase. Our objective was to estimate the degree to which climate change-driven shifts in water temperature may increase the exposure of West Virginia's native freshwater fishes to mountaintop removal surface coal mining. Mid-century shifts in habitat suitability for nine non-game West Virginia fishes were projected via Maximum Entropy species distribution modeling, using a combination of physical habitat, historical climate conditions, and future climate data. Modeling projections for a high-emissions scenario (Representative Concentration Pathway 8.5) predict that habitat suitability will increase in high elevation streams for eight of nine species, with marginal increases in habitat suitability ranging from 46-418%. We conclude that many West Virginia fishes will be at risk of increased exposure to mountaintop removal surface coal mining if climate change continues at a rapid pace.

Introduction

Quantifying and predicting species' responses to climate change is an active area of research in biogeographical and conservation science (e.g., Moritz et al. 2008; Angert et al. 2011; Newman et al. 2011). In the Northern Hemisphere, species are responding by shifting their ranges to the north or to higher elevations (e.g., Hickling et al. 2006; Chen et al. 2011; Comte & Grenouillet 2013). These latitudinal and elevational range shifts may be a result of species 'tracking' their thermal niches as temperatures in their historical, native ranges increase (Parmesan 2006; Comte et al. 2013; Freeman & Class Freeman 2014). If so, range shifts should be most likely for vagile species that are physically capable of long-distance movements and for ectothermic species that have narrow thermal tolerances (Calosi et al. 2008; Deutsch et al. 2008).

Freshwater fishes of the central Appalachian region, eastern North America, may be particularly likely to shift to higher elevations in response to a warming climate. Like most primary freshwater fishes, they are obligate ectotherms that may encounter stressful or lethal conditions as ambient temperatures increase (see Farrell 2011). Furthermore, most rivers in this region have a primarily east-west orientation; they flow off the Appalachian range west to the Ohio River, which is also a predominantly westward flowing river that originates near the Pennsylvania-New York border (~42 N latitude), or they flow east to the Atlantic Ocean. Thus, the topography and elevation of the Appalachian range may provide opportunities for freshwater fishes to shift their ranges upslope, while latitudinal shifts to the north will not be feasible for many populations.

Unfortunately, fishes that shift to higher elevations in central Appalachia will often encounter another threat: increased exposure to mountaintop removal (MTR) surface coal mining. Mountaintop removal mining is pervasive throughout central Appalachia and is particularly common in the state of West Virginia. Damages to aquatic biota may occur through acute loss of headwater streams (via burial by valley fill) or chronic degradation of water quality and instream habitat further downstream (Bernhardt et al. 2012). Empirical reports of MTR impacts on native fishes range from the individual-level toxic effects of selenium, a common byproduct of MTR that causes teratogenic deformities (Lemly 1993; Palmer et al. 2010), to assemblage-level effects including decreased species richness and lower population densities (Hitt and Chambers 2015). Habitat models also suggest that MTR may have a 'repulsive' effect on fish distributions, pushing them further downstream (Hopkins and Roush 2013).

In this study, we used Maximum Entropy (MaxEnt) species distribution models (SDMs) to assess whether climate change and MTR may pose an interactive threat to the native fishes of West Virginia. This was a two-step process in which we first used physical habitat and historical climate data to build SDMs for a subset of the native fishes of West Virginia. We then predicted future habitat suitability under two mid-century climate change scenarios. For each species and future climate scenario, we assessed changes in habitat suitability for streams in close proximity to MTR operations. However, our intent was not to model the effects of MTR on West Virginia fishes *per se*. Instead, we characterized the degree to which climate change may increase fish exposure to MTR via warming-induced upslope range shifts. Notably, our analyses focused on a subset of non-game fishes. Other investigators have studied climate change and MTR effects on West Virginia game fishes, such as Brook Trout (*Salvelinus fontinalis* Mitchell; e.g., Ries and Perry 1995), but little is known about the potential consequences for the region's diverse non-game fishes.

Specific research objectives were to: (i) build SDMs for nine non-game fish species that are broadly representative of the native ichthyofauna of West Virginia; (ii) predict changes in habitat suitability under two mid-century climate scenarios; and (iii) use the projected habitat suitability maps to identify species that are likely to migrate to higher elevations, thereby increasing their exposure to MTR.

Methods

Fish Data

We selected nine non-game fish species from the families Catostomidae, Cottidae, Cyprinidae, and Percidae. These four families constitute the majority of native fish diversity in West Virginia and an abundance of occurrence records were available for species in each family. Within families, species were selected at random and in proportion to the overall richness of the respective family. For instance, four species were selected from Cyprinidae, the most diverse family, but only two species were selected from the less diverse Catostomidae. Presence-only occurrence records for each of the nine species were obtained from the spatially-explicit Ichthymaps digital database (Frimpong et al. 2016). Notably, we included occurrence records throughout the entire Ohio River Basin, the parent drainage to most West Virginia rivers. Incorporating species' complete ranges throughout the Ohio River Basin, rather than truncated ranges within West Virginia, ensured that the MaxEnt 'background' samples (see 'Species Distribution Models' below) would be representative of all habitats available to the modeled species. This was important because an incomplete background sample can generate strong bias in MaxEnt results (Elith et al. 2011). To account for potential spatial bias in the Ichthymaps occurrence records (e.g., spatial clustering in the locations of samples that are close to a university), we applied a spatial thinning algorithm to the occurrence data. Using the spThin package in R (Aiello-Lammens et al. 2015), we applied a nearest neighbor search radius of 10 km to each Ichthymaps occurrence record. Fewer than 2% of all occurrence points were within 10 linear km of each other. We therefore concluded that geographic sampling bias was not a significant concern and retained all of the occurrence data in model development.

River Network, Physical Habitat, and Climate Data

The 1:100,000 scale National Hydrography Dataset Plus, Version 2 (NHDplus V2; McKay et al. 2012) digital stream network, clipped to the Ohio River Basin, was used as a common physical template for all fish occurrence records, environmental covariates (i.e., predictor variables), and SDMs. In the NHDplus V2, every digital stream segment has a unique 'COMID' identifier; these COMIDs were used to cross-reference all fish occurrence and covariate data to their respective locations within the Ohio River Basin. Physical habitat covariates were obtained from the NHDplus V2 attribute tables and the Stream-Catchment dataset (StreamCat; Hill et al. 2016). These physical habitat covariates were selected to represent four broad classes of potential effects on fish habitat: topographic, geologic, hydrologic, or urban. For example, select topographic covariates included elevation, channel slope, and catchment area, while urban covariates included dams and roads.

Historical (1960-1990) and mid-century (2041-2060) climate data were downloaded from WorldClim, Version 1.4 (Hijmans et al. 2005), as 30 arc-second resolution grids. Mid-century data were obtained for two Representative Concentration Pathway scenarios (RCPs): RCP 4.5 served as a mid-range emissions scenario (Thomson et al. 2011) and RCP 8.5 served as a high range emissions scenario (Riahi et al. 2011). The RCP 4.5 climate scenario is characterized by a divergence from fossil fuel use and an increase in sustainable land-use; this scenario estimates a 2.4° C mean temperature increase beyond pre-industrial levels (Thomson et al. 2011). Alternatively, the RCP 8.5 climate scenario is an increasing emissions pathway which assumes increased fossil fuel use and no climate change mitigation (Riahi et al. 2011); this scenario is characterized by a mean temperature increase of 4.9° C above pre-industrial levels (Raftery et al. 2017). For both RCPs, mid-century projections were downloaded for six general circulation models: BCC-CSM1-1 (Wu et al. 2014), CCSM4 (Gent et al. 2011), GFDL-CM3 (Donner et al. 2011), GISS-E2-R (Schmidt et al. 2014), HadGEM2-CC (Martin et al. 2011), and MRI-CGCM3 (Yukimoto et al. 2012). All climate grids were then re-projected to a common 1 km resolution grid spanning the entire Ohio River Basin. Next, ensemble mean averages were calculated for monthly air temperature and monthly precipitation in each 1 km grid cell (i.e., 12 monthly air temperature and precipitation values in each cell), under both RCP 4.5 and RCP 8.5. All grid calculations were performed with ESRI ArcMap 10.5 software (Environmental Systems Research Institute, Redlands, California). Gridded air temperature and precipitation values were then appended to the NHDplus V2 stream network by superimposing the climate grids directly onto the digital stream network, using System for Automated Geoscientific Analyses Version 2.1.4 software (Institute of Geography, Physical Geography Section, Hamburg University). From these data, we calculated mean annual streamflow for every digital stream segment in the Ohio River Basin using the Ohio River Basin-specific linear regression model of Vogel et al. (1999); their model predicts discharge as a linear function of drainage area, precipitation, and air temperature. We then calculated mean annual stream temperature using the logistic regression model of Segura et al. (2015); their model predicts stream temperature as a sigmoid function of air temperature.

Finally, we generated a Pearson correlation (*r*) matrix for all of the NHDplus V2, StreamCat, and derived climate variables (discharge and stream temperature) and used it to screen highly correlated covariates ($|r| \geq 0.70$) from the models. From the remaining variables, a subset of 30 covariates that are potentially relevant to freshwater fishes was selected (see Table 1 for the complete covariate list with definitions and units of measure).

Species Distribution Models

MaxEnt (American Museum of Natural History, New York, New York) was used to build the SDMs because it outperforms other modeling techniques when working with presence-only data, rather than presence-absence data (Elith et al. 2006). A complete discussion of the MaxEnt algorithm and why it is uniquely suited to presence-only data is beyond the scope of this article. Interested readers should consult the excellent tutorial of Phillips (2017) and the methodological reviews of Elith et al. (2011) and Merow et al. (2013). Here, we present only the settings and outputs that are necessary to critique or duplicate our SDMs. However, we note that our models used the MaxEnt 'raw' output, rather than the logistic output. MaxEnt raw output is an index of habitat suitability; values can range from zero (categorically unsuitable habitat) to a theoretical maximum of one (the best possible habitat), though in practice, most values will be much smaller than one because the raw output values across all habitat units used to fit the model must sum to one. MaxEnt logistic output is interpreted as the probability of presence, ranging from 0-1. Logistic output is often used because it is intuitively similar to logistic regression. Unfortunately, MaxEnt logistic output requires independent information on species' detection probabilities; without this information, MaxEnt uses default settings (that are not appropriate for many datasets) to generate logistic output (Elith et al. 2011). We lacked estimates of species' detection probabilities for the Ichthymaps samples and therefore did not use the MaxEnt logistic output.

Briefly, our modeling process was as follows (see Figure 1). Historical species occurrence and environmental covariate data were used to build a MaxEnt model for each of the nine fishes. For each modeled species, a 'background' sample was created by randomly selecting 20% of the complete landscape (i.e., 20% of all NHDplus V2 stream segments within the Ohio River Basin). This was necessary to implement the core MaxEnt logic of comparing covariate values at known occurrence sites (i.e., the 'sample' distribution) with a random sample of background sites (see description of the MaxEnt 'regularized training gain' below). To avoid overfitting the models and to ease interpretation of individual covariate effects, we constrained the MaxEnt models to simple hinge and quadratic features (see Elith et al. 2011).

An iterative process was then used with standard MaxEnt diagnostics to sort through the 30 potential covariates and select those that were the most effective predictors of a given species' occurrence. These diagnostics included the MaxEnt percent contribution and permutation importance summary tables for individual covariates as well as the covariate jackknife plots. Percent contribution is a heuristic estimate of the relative contribution of each covariate that is included in a model; larger values indicate covariates that contribute more information. Similarly, permutation importance is greatest for covariates that contribute the most information; it is a measure of the change in model fit when values of a given covariate are randomly shuffled among sites. Jackknife plots illustrate the effect of a given covariate by showing the change in model fit when that covariate is removed from the model; a large change indicates a covariate that contributes a relatively large amount of information to the model.

The MaxEnt regularized training gain was used as an index of model fit. Regularized training gain is a measure of the distance between a multivariate distribution of covariates at randomly selected background sites (i.e., a random sample of the entire landscape that a species could potentially inhabit) and a corresponding distribution of covariates at sites of known species occurrences (Elith et al. 2011). Hence, a large training gain indicates an affinity for a narrow range of environmental conditions, relative to the broader landscape, while a small training gain suggests a lack of specialized habitat requirements (i.e., the distribution of covariates at occurrence sites mirrors the background distribution; Merow et al. 2013). We also used the exponential transformation of the MaxEnt regularized training gain for each SDM to aid in model evaluation. The exponential of the regularized training gain is the ratio of habitat suitability between sites of known occurrence and randomly selected background sites. Exponential values much larger than one are indicative of species with specialized habitat requirements; because these specialist species occupy a narrow range of habitats, relative to the complete range of available habitats, SDMs can more efficiently discriminate between suitable and unsuitable habitat.

Once a final MaxEnt model had been specified for each of the nine fish species, habitat suitability was projected to a mid-century time horizon (2014-2060) under the RCP 4.5 and RCP 8.5 climate change scenarios. This was accomplished by substituting future values of the climate-driven covariates (streamflow, stream temperature, and precipitation) for the historical values used to build and parameterize each model. Then, by comparing aggregate distributions of

MaxEnt raw output values among historical and future landscapes, we were able to estimate potential shifts in habitat suitability for each fish species.

Finally, we used a spatial querying process to identify stream segments that are likely to be impacted by MTR operations in the state of West Virginia. We began with a digital map of all active MTR permit boundaries from the West Virginia Department of Environmental Protection (http://tagis.dep.wv.gov/home/Downloads; downloaded on 24 October 2017). A 10 km radial buffer was then built around each of the MTR sites in ArcMap. The 10 km buffer provided an estimate of the potential 'spatial footprint' of MTR effects on local aquatic ecosystems; in several instances, significant effects of MTR on aquatic biota have been documented at downstream distances >10 km (e.g., Pond et al. 2008; Lindberg et al. 2011; Bernhardt et al. 2012). By using the MTR buffer to query potentially impacted stream reaches from the complete river network, we were able to test the hypothesis that climate change is likely to increase exposure of West Virginia fishes to MTR.

Comparisons between historical and future SDM projections were made using the nonparametric one-sided Mann-Whitney U test. This test compares the distribution of ranks between two unpaired datasets. The datasets are combined and each value is ranked from smallest to largest. From this rank distribution, the average ranks of the members of each group are calculated; a large difference between the groups' mean ranks suggests the distributions are distinct. The U-statistic indicates how often the rank of a member of one group exceeds the rank of a member of the second group.

Results

Complete MaxEnt results for each of the nine species, including sample sizes, model fit diagnostics, and indices of importance for individual covariates, are shown in Table 2. Summary statistics for all MaxEnt habitat suitability predictions are illustrated in Figure 2. Under the RCP 4.5 climate scenario, significant increases (Mann-Whitney: $P < 0.001$) in habitat suitability were predicted within the MTR buffer for the two darters (Etheostoma), but none of the remaining species (Figure 2). However, under the RCP 8.5 scenario, habitat suitability was predicted to significantly increase within the MTR buffer for eight of nine species (Table 3). Among RCP 8.5 projections, these increases ranged from +46% to +418%, relative to the historical habitat suitability values, with a median increase of +125% (Table 3). Only the Silverjaw Minnow (*Notropis buccatus* Cope) was predicted to experience a decrease in habitat suitability within the MTR buffer. Differences in MaxEnt predicted habitat suitability among the RCP 4.5 and RCP 8.5 mid-century scenarios are illustrated in Figure 3 using the Striped Shiner (*Luxilus chrysocephalus* Rafinesque) as an example.

Discussion

Our results generally support the hypothesis that directional range shifts in response to climate change among West Virginia's freshwater fishes will occur as upslope shifts to high elevation streams. Under the RCP 8.5 climate scenario, habitat suitability is likely to increase for eight of nine species in streams in close proximity to MTR; percent change in suitability exceeds +100% for several species. Results are more nuanced for streams within the MTR buffer under the RCP 4.5 scenario; some species are projected to experience reduced habitat suitability while for other species suitability is estimated to increase. Expected shifts in habitat suitability across the Ohio River Basin mirror the shifts projected for streams within the MTR buffer. In general, under the RCP 4.5 scenario suitability across the Ohio River Basin shifts minimally. Under the RCP 8.5 scenario, increased habitat suitability is estimated for most species, though shifts are considerably smaller than shifts expected within the MTR buffer.

Under the RCP 4.5 climate scenario, the Greenside Darter (*Etheostoma blennioides* Rafinesque) and the Rainbow Darter *(Etheostoma caeruleum* Storer) are projected to experience shifts in habitat suitability of +19% and +29% within the MTR buffer, respectively. Interestingly, the darters (Etheostoma) are the only species expected to experience increases in suitability within the MTR buffer under the low emissions scenario (Table 3). Models for both species included mean annual streamflow and mean January precipitation (Table 2). Potentially, historic hydrological conditions approached the lower bound of the physiological threshold of the Greenside and Rainbow Darters. Therefore, changes in streamflow and precipitation under the RCP 4.5 scenario would benefit the species. Projected increases in habitat suitability within the MTR buffer are even greater for the Greenside Darter (+119%) and Rainbow Darter (+154%) under the RCP 8.5 climate scenario. Conversely, the Silverjaw Minnow is the only species predicted to experience declining habitat suitability within the MTR buffer under RCP 8.5 (Table 3). This reverse trend in suitability may indicate that the functional thresholds of the Silverjaw Minnow will be exceeded under either climate scenario. For this species, projected shifts in habitat suitability within the MTR buffer are -33% and -31% for RCP 4.5 and RCP 8.5, respectively. However, the distribution of raw scores between historical and RCP 4.5 and RCP 8.5 scenarios were not significantly different (Figure 2). The Silverjaw Minnow model included runoff, mean annual streamflow, and January and June precipitation (Table 2). Thus, hydrological changes under the RCP 4.5 and RCP 8.5 climate scenarios are expected to exacerbate historically unsuitable conditions for the Silverjaw Minnow. This reserve trend in suitability persisted across the Ohio River Basin.

Climate Change Effects — Flow vs Temperature

Because ambient temperature is a primary determinant of habitat suitability for ectotherms, we expected stream temperature to be an important predictor of fish species presence (Deutsch et al. 2008; Coulter et al. 2014). Surprisingly, this was not the case; stream temperature was not included in any of the final models (see Table 2). Nevertheless, our results suggest that aquatic habitat in upslope, high elevation streams is likely to become more suitable by mid-century, particularly under an RCP 8.5 climate scenario.

The apparent lack of a strong temperature effect may be a result of the modeled species having broad thermal tolerances. At historical occurrence sites, the widest ranges of winter and summer stream temperature values for a given species (i.e., stream temperature ranges among all sites of known presence) spanned 2.74° C (Creek Chub (*Semotilus atromaculatus* Mitchell); min. = 0.38° C; max. = 3.12° C) and 6.24° C (Silverjaw Minnow; min. = 22.72° C; max. = 28.96° C), respectively. Conversely, the narrowest ranges of historical winter and summer stream temperatures for a given species spanned 2.62° C (Striped Shiner; min. = 0.40° C; max. = 3.02° C) and 5.53° C (Mottled Sculpin (*Cottus bairdii* Girard); min. = 23.36° C; max. = 28.89° C), respectively. In all cases, species' historical winter and summer temperature ranges encompassed a large fraction of the historical temperature range across the entire Ohio River Basin: historical winter and summer stream temperatures spanned 2.76° C (min. = 0.36° C; max. = 3.12° C) and 6.32° C (min. = 22.69° C; max. = 29.01° C), respectively. Together, these observations suggest that each of the nine modeled fishes would be physiologically capable of occupying most or all of the streams in the Ohio River Basin, if mean winter or summer stream temperature were the sole determinant of habitat suitability. The fact that documented occurrences of each of the modeled species were limited to a subset of streams within the Ohio Basin suggests that other factors than stream temperature are fundamental in regulating fish species' presences. With specific reference to MaxEnt, the fact that historical sample temperatures exhibit so much overlap with the background temperatures indicates that mean winter and summer stream temperatures may not be useful for discriminating between suitable and unsuitable fish habitat.

Instead, species' responses to climate change were driven primarily by hydrology. In each model, hydrologic variables were among the best predictors of fish occurrence (Table 2). For example, mean annual streamflow was included in every model and in eight of nine cases, it was the first or second best covariate when ranked by MaxEnt percent contribution statistics (13.5-42.4%). Other covariates that represent hydrology or a dimension of the hydrologic cycle included summer and winter precipitation (one of which was included in every model), runoff (included in eight of nine models), and the baseflow index (included in six models). Importantly, these differing hydrology covariates did not provide redundant information. When calculated across the entire Ohio River Basin, Pearson correlation coefficients among these covariates never exceeded the collinearity threshold of $|r| > 0.70$ and in several instances, were much lower. For instance, correlations between mean annual streamflow and January precipitation, and between streamflow and June precipitation were $r < 0.01$ and $r = -0.40$, respectively. Furthermore, January and June precipitation were not highly correlated ($r = 0.35$). Thus, we concluded that the various hydrologic covariates (streamflow, precipitation, runoff, baseflow index) represented different dimensions of the hydrologic cycle and were therefore appropriate for inclusion in the same models.

In retrospect, the strong effect of hydrology was not surprising, given that hydrology is widely regarded as a “master” variable in lotic ecosystems (Poff et al. 1997). Streamflow is a dynamic integration of many physical processes occurring across the landscape. Though it is clearly a function of precipitation, streamflow is also influenced by the geologic and antecedent factors that regulate surface runoff, soil water, and groundwater dynamics (Poff et al. 1997). In this way, streamflow becomes an efficient indicator of many different yet interrelated influences on aquatic habitat (McGarvey and Terra 2016). Effects of these hydrologic influences range from direct, individual-level physiological and behavioral mechanisms (Poff and Allan 1995; Poff et al. 1997; Mims and Olden 2011) to emergent patterns in species’ distributions and overall richness (Power et al. 1995; Wenger et al. 2011; McGarvey 2014). We therefore believe it is logical that streamflow, rather than stream temperature, proved to be a primary determinant of habitat suitability in the fish models.

Are the Model Predictions Cause for Concern?

Our results suggest that, in a warming climate, habitat suitability for eight of the nine modeled species is likely to increase in high elevation streams near MTR operations. But we cannot prove that any of our predicted changes in habitat suitability will come to pass, or that the study species will in fact migrate to streams within the MTR buffer. We therefore conclude with some general thoughts on the relevance of our modeling process and findings.

First, we emphasize that the RCP 4.5 and 8.5 climate change scenarios, though heuristic in nature, are broadly recognized by the scientific community as valid and entirely plausible. Indeed, Smith et al. (2011) have shown that global warming of 2° C beyond pre-industrial levels may be achieved as early as 2030 and that 4° C warming may occur as soon as 2060. Similarly, Betts et al. (2011) estimate global mean temperature will increase by 4° C above pre-industrial levels between 2060-2070. Others propose global mean temperature is highly likely to exceed the 2° C benchmark by 2030, citing a likely temperature increase that ranges from 2-4.9° C by 2100 (Raftery et al. 2016). Collectively, these reports show, despite uncertainty, that the range of outcomes bracketed by the RCP 4.5 and RCP 8.5 climate scenarios are plausible and could be reached by mid-century.

Second, there are relatively few migration barriers in the rivers and streams of West Virginia that would categorially prevent fishes from migrating to higher elevations near MTR sites. Numerous lock-and-dam structures exist along the mainstem Ohio, Kanawha, and Monongahela Rivers in West Virginia but these are permeable to fish movement and the number of large impassible dams on westward flowing, Ohio River tributaries is modest in comparison to other eastern U.S. states (USACE 2016). Using a GIS, we performed a manual search for large dams that would prevent upstream fish movement and identified 10: Hawks Nest (inclusive of all upstream dams on the mainstem New River), Summersville, Sutton, Taylor Fork, Shannonpin Mine, Cheat Lake, Tygart, R.D. Bailey, Upper Mud River No. 2A, and East Lynn. The total length of stream channel that was upstream of one of these dams and within the MTR buffer was 1,440 km, or ~9% of the 15,732 km of total stream channel within the buffer. Less conspicuous barriers could also constrain future fish movement. For instance, road crossings and culverts often impede fish movement (Warren and Pardew 1998; Januchowski-Hartley et al. 2013). This is a point of concern because the density of road crossings was a good predictor of fish occurrence, and therefore selected as a final predictor variable, for eight of the nine modeled species (Table 2). Currently, we do not have comprehensive data that could be used to incorporate road crossings into our analyses in a spatially explicit manner. But we do note that most of the fishes in this study have broad ranges that historically include some mid- to high-elevation streams. Thus, it is likely that even in a landscape that is highly fragmented by road crossings, some potential colonists are already present near the MTR buffer sites and therefore capable of moving to them in a changing climate.

Third, we submit that our specific results may be broadly representative of a large fraction of the complete, native ichthyofauna of West Virginia. Our study species were randomly selected from the families Catostomidae, Cottidae, Cyprinidae, and Percidae. Together, these four families include 114 non-game fish species and represent 64% of all native fishes in West Virginia. As noted above, the model-predicted shifts in high-elevation habitat suitability were generally positive (i.e., increasing suitability) for eight of nine species. Thus, we believe it is logical to predict that habitat suitability for many of the remaining fishes will respond in a similar manner.

Finally, although we did not model MTR effects on fishes *per se*, we posit that the predicted tendency for habitat suitability to increase near MTR sites is, of itself, legitimate cause for concern. The most acute, negative effect of MTR on freshwater fishes will be direct habitat loss as MTR overburden is dumped as valley-fill, effectively eliminating headwater streams. Further downstream, chemical contaminants will accumulate through leaching and as coal is washed to lower its sulfur-content. Toxicants from MTR are known to cause infertility (Palmer et al. 2010), teratogenic deformities (Palmer et al. 2010), and death among individual fishes

(Ferreri et al. 2004), as well as population- and assemblage-level declines in fish abundance and diversity (Ferreri et al. 2004; Hitt and Chambers 2015). In southern West Virginia, more than 750 km of high elevation streams have already been buried by MTR waste and chronic effects of MTR are now impacting 2800-4300 km of additional stream habitat (Bernhardt et al. 2012). Thus, we conclude that the combined effects of climate change and MTR are likely to pose very real and significant threats to many of West Virginia's native freshwater fishes by mid-century.

Acknowledgements

L. Hendrick received financial support through the Virginia Commonwealth University Rice Rivers Center. D. McGarvey received financial support through the National Science Foundation (DEB-1553111) and the Eppley Foundation for Scientific Research.

References

Aiello-Lammens, M. E., R. A. Boria, A. Radosavljevic, B. Vilela, and R. P. Anderson. 2015. spThin: An R package for spatial thinning of species occurrence records for use in ecological niche models. Ecography 38(5):541–545.

Angert, A. L., L. G. Crozier, L. J. Rissler, S. E. Gilman, J. J. Tewksbury, and A. J. Chunco. 2011. Do species' traits predict recent shifts at expanding range edges? Ecology Letters 14:677–689.

Bernhardt, E. S., B. D. Lutz, R. S. King, J. P. Fay, C. E. Carter, A. M. Helton, D. Campagna, and J. Amos. 2012. How many mountains can we mine? Cumulative impacts of surface coal mining on Central Appalachian rivers. Environmental Science & Technology 46:8115–8122.

Betts, R. A., M. Collins, D. L. Hemming, C. D. Jones, J. A. Lowe, and M. G. Sanderson. 2011. When could global warming reach 4° C? Philosophical Transactions of the Royal Society A: Mathematical, Physical and Engineering Sciences 369(1934):67–84.

Calosi, P., D. T. Bilton, and J. I. Spicer. 2008. Thermal tolerance, acclimatory capacity and vulnerability to global climate change. Biology Letters 4(1):99–102.

Chen, I. C., J. K. Hill, R. Ohlemüller, D. B. Roy, and C. D. Thomas. 2011. Rapid range shifts of species associated with high levels of climate warming. Science 333(6045):1024–1026.

Comte, L., L. Buisson, M. Daufresne, and G. Grenouillet. 2013. Climate-induced changes in the distribution of freshwater fish: Observed and predicted trends. Freshwater Biology 58(4):625–639.

Comte, L., and G. Grenouillet. 2013. Do stream fish track climate change? Assessing distribution shifts in recent decades. Ecography 36(11):1236–1246.

Coulter, D. P., M. S. Sepúlveda, C. D. Troy, and T. O. Höök. 2014. Thermal habitat quality of aquatic organisms near power plant discharges: Potential exacerbating effects of climate warming. Fisheries Management and Ecology 21(3):196-210.

Deutsch, C. A., J. J. Tewksbury, R. B. Huey, K. S. Sheldon, C. K. Ghalambor, D. C. Haak, and P. R. Martin. 2008. Impacts of climate warming on terrestrial ectotherms across latitude. Proceedings of the National Academy of Sciences 105(18):6668–6672.

Donner, L. J., B. L. Wyman, R. S. Hemler, L. W. Horowitz, Y. Ming, M. Zhao, J. C. Golaz, P. Ginoux, S. J. Lin, M. D. Schwarzkopf, J. Austin, G. Alaka, W. F. Cooke, T. L. Delworth, S. M. Freidenreich, C. T. Gordon, S. M. Griffies, I. M. Held, W. J. Hurlin, S. A. Klein, T. R. Knutson, A. R. Langenhorst, H. C. Lee, Y. Lin, B. I. Magi, S. L. Malyshev, P. C. D. Milly, V. Naik, M. J. Nath, R. Pincus, J. J. Ploshay, V. Ramaswamy, C. J. Seman, E. Shevliakova, J. J. Sirutis, W. F. Stern, R. J. Stouffer, R. J. Wilson, M. Winton, A. T. Wittenberg, and F. Zeng. 2011. The dynamical core, physical parameterizations, and basic simulation characteristics of the atmospheric component AM3 of the GFDL global coupled model CM3. Journal of Climate 24(13):3484–3519.

Elith, J., C. H. Graham, R. P. Anderson, M. Dudik, S. Ferrier, A. Guisan, R. J. Hijmans, F. Huettmann, J. R. Leathwick, A. Lehmann, J. Li, L. G. Lohmann, B. A. Loiselle, G. Manion, C. Moritz, M. Nakamura, Y. Nakazawa, J. M. Overton, A. T. Peterson, S. J. Phillips, K. Richardson, R. Scachetti-Pereira, R. E. Schapire, J. Soberon, S. Williams, M. S. Wisz, and N. E. Zimmermann. 2006. Novel methods improve prediction of species’ distributions from occurrence data. Ecography 29(2):129–151.

Elith, J., S. J. Phillips, T. Hastie, M. Dudík, Y. E. Chee, and C. J. Yates. 2011. A statistical explanation of MaxEnt for ecologists. Diversity and Distributions 17(1):43–57.

Farrell, A. P., editor. 2011. Encyclopedia of fish physiology: from genome to environment, 1st edition. Elsevier, London.

Ferreri, C. P., J. R. Stauffer, and T. D. Stecko. 2004. Evaluating Impacts of Mountain Top Removal / Valley Fill Coal Mining on Stream Fish Populations. Pages 576–592 in Proceedings of the National Meeting of the American Society of Mining and Reclamation and the 25th West Virginia Surface Mine Drainage Task Force, April 18-24, 2004. Lexington, KY.

Freeman, B. G., and A. M. Class Freeman. 2014. Rapid upslope shifts in New Guinean birds illustrate strong distributional responses of tropical montane species to global warming. Proceedings of the National Academy of Sciences 111(12):4490–4494.

Frimpong, E. A., J. Huang, and Y. Liang. 2016. IchthyMaps: A Database of Historical Distributions of Freshwater Fishes of the United States. Fisheries 41(10):590–599.

Gent, P. R., G. Danabasoglu, L. J. Donner, M. M. Holland, E. C. Hunke, S. R. Jayne, D. M. Lawrence, R. B. Neale, P. J. Rasch, M. Vertenstein, P. H. Worley, Z. L. Yang, and M. Zhang. 2011. The community climate system model version 4. Journal of Climate 24(19):4973–4991.

Hickling, R., D. B. Roy, J. K. Hill, R. Fox, and C. D. Thomas. 2006. The distributions of a wide range of taxonomic groups are expanding polewards. Global Change Biology 12(3):450–455.

Hijmans, R. J., S. E. Cameron, J. L. Parra, P. G. Jones, and A. Jarvis. 2005. Very high resolution interpolated climate surfaces for global land areas. International Journal of Climatology 25(15):1965–1978.

Hill, R. A., M. H. Weber, S. G. Leibowitz, A. R. Olsen, and D. J. Thornbrugh. 2016. The Stream-Catchment (StreamCat) Dataset: A Database of Watershed Metrics for the Conterminous United States. Journal of the American Water Resources Association 52(1):120–128.

Hitt, N. P., and D. B. Chambers. 2015. Temporal changes in taxonomic and functional diversity of fish assemblages downstream from mountaintop mining. Freshwater Science 33(3):915–926.

Hopkins, R. L., and J. C. Roush. 2013. Effects of mountaintop mining on fish distributions in central Appalachia. Ecology of Freshwater Fish 22(4):578–586.

Januchowski-Hartley, S. R., P. B. McIntyre, M. Diebel, P. J. Doran, D. M. Infante, C. Joseph, and J. D. Allan. 2013. Restoring aquatic ecosystem connectivity requires expanding inventories of both dams and road crossings. Frontiers in Ecology and the Environment 11(4):211–217.

Lemly, A. D. 1993. Teratogenic effects of selenium in natural populations of freshwater fish. Ecotoxicology and Environmental Safety 26(3):181–204.

Lindberg, T. T., E. S. Bernhardt, R. Bier, A. M. Helton, R. B. Merola, A. Vengosh, and R. T. Di Giulio. 2011. Cumulative impacts of mountaintop mining on an Appalachian watershed. Proceedings of the National Academy of Sciences 108(52):20929–20934.

Martin, G. M., N. Bellouin, W. J. Collins, I. D. Culverwell, P. R. Halloran, S. C. Hardiman, T. J. Hinton, C. D. Jones, R. E. McDonald, A. J. McLaren, F. M. O'Connor, M. J. Roberts, J. M. Rodriguez, S. Woodward, M. J. Best, M. E. Brooks, A. R. Brown, N. Butchart, C. Dearden, S. H. Derbyshire, I. Dharssi, M. Doutriaux-Boucher, J. M. Edwards, P. D. Falloon, N. Gedney, L. J. Gray, H. T. Hewitt, M. Hobson, M. R. Huddleston, J. Hughes, S. Ineson, W.

J. Ingram, P. M. James, T. C. Johns, C. E. Johnson, A. Jones, C. P. Jones, M. M. Joshi, A. B. Keen, S. Liddicoat, A. P. Lock, A. V. Maidens, J. C. Manners, S. F. Milton, J. G. L. Rae, J. K. Ridley, A. Sellar, C. A. Senior, I. J. Totterdell, A. Verhoef, P. L. Vidale, and A. Wiltshire. 2011. The HadGEM2 family of Met Office Unified Model climate configurations. Geoscientific Model Development 4:723–757.

McGarvey, D. J. 2014. Moving beyond species – discharge relationships to a flow-mediated , macroecological theory of fish species richness. Freshwater Science 33(1):18–31.

McGarvey, D. J., and B. de F. Terra. 2016. Using river discharge to model and deconstruct the latitudinal diversity gradient for fishes of the Western Hemisphere. Journal of Biogeography 43(7):1436–1449.

McKay, L., T. Bondelid, T. Dewald, J. Johnston, R. Moore, and A. Rea. 2012. NHD Plus Version 2: User Guide.

Merow, C., M. J. Smith, and J. A. Silander. 2013. A practical guide to MaxEnt for modeling species' distributions: What it does, and why inputs and settings matter. Ecography 36(10):1058–1069.

Mims, M. C., and J. D. Olden. 2012. Life history theory predicts fish assemblage response to hydrologic regimes. Ecology 93(1):35–45.

Moritz, C., J. L. Patton, C. J. Conroy, J. L. Parra, G. C. White, and S. R. Beissinger. 2008. Impact of a century of climate change on small-mammal communities in Yosemite National Park, USA. Science 322:261–264.

Newman, J. A., M. Anand, A. L. Hugh, S. Hunt, and Z. Gedalof. 2011. Climate Change Biology. CAB International, Cambridge.

Palmer, M. A., E. S. Bernhardt, W. H. Schlesinger, K. N. Eshleman, E. Foufoula- Georgiou, M.

S. Hendryx, A. Lemly, G. E. Likens, O. L. Loucks, M. E. Power, P. S. White, and P. R. Wilcock. 2010. Mountaintop Mining Consequences. Science 327:148–149.

Parmesan, C. 2006. Ecological and Evolutionary Responses to Recent Climate Change. Annual Review of Ecology, Evolution, and Systematics 37(1):637–669.

Phillips, S. J. 2017. A brief tutorial in Maxent. Available: https://biodiversityinformatics.amnh.org/open_source/maxent/. (February 2018).

Poff, N. L., and J. D. Allan. 1995. Functional organization of stream Fish Assemblages in Relation to Hydrological Variability. Ecology 76(2):606–627.

Poff, N. L., J. D. Allan, M. B. Bain, J. R. Karr, K. L. Prestegaard, B. D. Richter, R. E. Sparks, and J. C. Stromberg. 1997. The Natural Flow Regime. BioScience 47(11):769–784.

Pond, G. J., M. E. Passmore, F. A. Borsuk, L. Reynolds, and C. J. Rose. 2008. Downstream effects of mountaintop coal mining: comparing biological conditions using family- and genus-level macroinvertebrate bioassessment tools. Journal of the North American Benthological Society 27(3):717–737.

Power, M. E., A. Sun, G. Parker, W. E. Dietrich, J. T. Wootton, and J. T. Woott. 1995. Hydraulic Food-Chain Models - An approach to the study of food-web dynamics in large rivers. BioScience 45(3):159–167.

Raftery, A. E., A. Zimmer, D. M. W. Frierson, R. Startz, and P. Liu. 2017. Less than 2 °C warming by 2100 unlikely. Nature Climate Change 7(9):637–641.

Riahi, K., S. Rao, V. Krey, C. Cho, V. Chirkov, G. Fischer, G. Kindermann, N. Nakicenovic, and P. Rafaj. 2011. RCP 8.5-A scenario of comparatively high greenhouse gas emissions. Climatic Change 109(1):33–57.

Ries, R., and S. Perry. 1995. Potential effects of global climate change on brook trout growth and prey consumption incentral Appalachian streams, USA. Climate Research 5(3):197–206.

Schmidt, G. A., M. Kelley, L. Nazarenko, R. Ruedy, G. L. Russell, I. Aleinov, M. Bauer, S. E. Bauer, M. K. Bhat, R. Bleck, V. Canuto, Y. Chen, Y. Cheng, T. L. Clune, A. Del Genio, R. De Fainchtein, G. Faluvegi, J. E. Hansen, R. J. Healy, N. Y. Kiang, D. Koch, A. A. Lacis, A. N. Legrande, J. Lerner, K. K. Lo, E. E. Matthews, S. Menon, R. L. Miller, V. Oinas, and A. O. Oloso. 2014. Journal of Advances in Modeling Earth Systems contributions to the CMIP5 archive. Journal of Advances in Modeling Earth Systems 6:141–184.

Segura, C., P. Caldwell, G. Sun, S. Mcnulty, and Y. Zhang. 2015. A model to predict stream water temperature across the conterminous USA. Hydrological Processes 29:2178–2195.

Smith, M. S., L. Horrocks, A. Harvey, and C. Hamilton. 2011. Rethinking adaptation for a 4 C world. Philosophical Transactions of the Royal Society A: Mathematical, Physical and Engineering Sciences 369(1934):196–216.

Thomson, A. M., K. V. Calvin, S. J. Smith, G. P. Kyle, A. Volke, P. Patel, S. Delgado-Arias, B. Bond-Lamberty, M. A. Wise, L. E. Clarke, and J. A. Edmonds. 2011. RCP4.5: A pathway for stabilization of radiative forcing by 2100. Climatic Change 109(1):77–94.

[USACE] U.S. Army Corps of Engineers. 2016. National Inventory of dams. Available: http://nid.usace.army.mil/cm_apex/f?p=838:12. (March 2018).

Vogel, R., I. Wilson, and C. Daly. 1999. Regional Regression Models of Annual Streamflow for the United States. Journal Of Irrigation and Drainage Engineering 125(3):148–157.

Warren, M. L., and M. G. Pardew. 1998. Road Crossings as Barriers to Small-Stream Fish Movement. Transactions of the American Fisheries Society 127(4):637–644.

Wenger, S. J., D. J. Isaak, C. H. Luce, H. M. Neville, K. D. Fausch, J. B. Dunham, D. C. Dauwalter, M. K. Young, M. M. Elsner, B. E. Rieman, A. F. Hamlet, and J. E. Williams.

2011. Flow regime, temperature, and biotic interactions drive differential declines of trout species under climate change. Proceedings of the National Academy of Sciences of the United States of America 108(34):14175–14180.

Wu, T., L. Song, W. Li, Z. Wang, H. Zhang, X. Xin, Y. Zhang, L. Zhang, J. Li, F. Wu, Y. Liu, F. Zhang, X. Shi, M. Chu, J. Zhang, Y. Fang, F. Wang, Y. Lu, X. Liu, M. Wei, Q. Liu, W. Zhou, M. Dong, Q. Zhao, J. Ji, L. Li, and M. Zhou. 2014. An Overview of BCC Climate System Model Development and Application for Climate Change Studies. Journal of Meteorological Research 28(1):34–56.

Yukimoto, S., Y. Adachi, M. Hosaka, T. Sakami, H. Yoshimura, M. Hirabara, T. Y. Tanaka, E. Shindo, H. Tsujino, M. Deushi, R. Mizuta, S. Yabu, A. Obata, H. Nakano, T. Koshiro, T. Ose, and A. Kitoh. 2012. A New Global Climate Model of the Meteorological Research Institute: MRI-CGCM3—Model Description and Basic Performance. Journal of the Meteorological Society of Japan 90A:23–64.

TABLES

Table 1. Subset of all NHDplus V2, StreamCat, and derived climate variables considered in the initial Maximum Entropy (MaxEnt) species distribution models.

Covariate	**Extent**	**Unit**	**Description**	**Source**
Area	Catchment	km^2	Area of local NHDplus catchment	StreamCat
Average wetness index	Catchment	-	Mean Composite Topographic Index(CTI)[Wetness Index] within the local catchment	StreamCat
Barren land 2011	Catchment	%	Percent of the local catchment classified as barren land and other areas of accumulations of earthen material in 2011	StreamCat
BFI	Catchment	%	The ratio of base flow to local flow within the local catchment	StreamCat
Catchment SiO_2	Catchment	%	Mean of all values of lithological silicon dioxide content in surface or near surface geology within the local catchment	StreamCat
Coal mines	Catchment	sites/km^2	Density of georeferenced coal mines within the local catchment	StreamCat
Crop land 2006	Catchment	%	Percent of the local catchment classified as row crop land cover in 2006	StreamCat
Elevation	Catchment	m	Mean of all elevation values within the local catchment	StreamCat
Fe_2O_3	Catchment	%	Mean of all values of lithological ferric oxide content in surface or near surface geology within the local catchment	StreamCat
Forest loss 2010	Catchment	%	% tree canopy cover loss in 2010 within the local catchment and within 100 m buffer of stream lines	StreamCat
January precipitation	Stream	mm	Mean monthly precipitation in January (1960-1990)	Hendrick
January stream temperature	Stream	C	Mean monthly stream temperature in January (1960-1990)	Hendrick
July stream temperature	Stream	C	Mean monthly stream temperature in July (1960-1990)	Hendrick
June precipitation	Stream	mm	Mean monthly precipitation in June (1960-1990)	Hendrick
Mines	Catchment	sites/km^2	Density of georeferenced mines and mineral plants within the local catchment	StreamCat
NABD	Catchment	dams/km^2	Density of georeferenced dams within the local catchment	StreamCat
Nitrogen	Catchment	%	Mean of all values of lithological nitrogen content in surface or near surface geology within the local catchment	StreamCat
NPDES	Catchment	sites/km^2	Density of georeferenced National Pollutant Discharge Elimination System sites in the local catchment	StreamCat
Open water 2006	Catchment	%	Percent of the local catchment classified as open water land cover in 2006	StreamCat
Organic matter	Catchment	%	Mean of all organic matter values within the local catchment	StreamCat
Road crossings	Catchment	crossing/km^2	Sum of all road and stream crossings within the local catchment	StreamCat
Roads	Catchment	km/km^2	Mean of all values of road density calculated using 2010 Census data within the local catchment	StreamCat
Runoff	Catchment	mm	Mean of all values of estimated runoff between 1971-2000 within the local catchment	StreamCat
Sand	Catchment	%	Mean of all sand values within the local catchment	StreamCat
Slope	Stream	m	Slope of flowline (meters/meters), based on smoothed elevations	NHDplus v2
Stream order	Stream	-	Modified Strahler Stream Order	NHDplus v2
Streamflow	Stream	m^3s/km	Mean annual streamflow (1960-1990)	Hendrick
Superfund	Catchment	sites/km^2	Density of georeferenced Superfund sites in the local catchment	StreamCat
TRI	Catchment	sites/km^2	Density of georeferenced Toxic Release Inventory sites in the local catchment	StreamCat
Water table depth	Catchment	cm	Mean of all water table depth values within the local catchment	StreamCat

Table 2. Summary information on the fit and structure of the Maximum Entropy (MaxEnt) species distribution models. For each species, the number of occurrence records (n) used to build the model and the MaxEnt regularized training gain (rtg) are shown with the exponential of the rtg in parentheses. MaxEnt % contribution and permutation importance diagnostics are also shown for each covariate that was retained in a species' final model.

Species	**Covariate**	**% contribution**	**Permutation importance**
Catostomidae			
Catostomus commersonii	Catchment area	41.8	54.9
n = 2478	Mean annual streamflow	24.4	12.0
rtg = 0.614 (1.848)	Mean June precipitation	11.7	11.7
	Catchment runoff	7.6	6.3
	Catchment road crossings	4.4	0.8
	Catchment BFI	4.2	2.8
	Catchment elevation	4.1	8.3
	Stream order	1.7	3.2
Hypentelium nigricans	Catchment area	47.8	55.4
n = 2716	Mean annual streamflow	31.6	26.4
rtg = 0.565 (1.759)	Catchment elevation	9.6	9.1
	Mean June precipitation	3.1	2.9
	Catchment road crossings	2.9	1.1
	Catchment BFI	2.7	2.6
	Catchment water table depth	2.3	2.4
Cottidae			
Cottus bairdii	Catchment BFI	18.0	7.4
n = 893	Catchment area	17.0	24.1
rtg = 1.166 (3.209)	Catchment elevation	16.7	28.5
	Catchment runoff	13.6	21.8
	Mean annual streamflow	13.5	9.4
	Catchment sand	9.0	4.5
	Catchment road crossings	6.5	1.0
	Mean June precipitation	5.7	3.2

Table 2 (continued)

Cyprinidae			
Campostoma anomalum	Catchment area	42.1	46.8
n = 3156	Mean annual streamflow	34.7	33.4
rtg = 0.540 (1.716)	Mean June precipitation	5.5	6.7
	Catchment elevation	5.2	6.6
	Catchment runoff	4.9	2.9
	Catchment road crossings	3.8	0.6
	Catchment BFI	2.4	1.0
	Catchment Fe_2O_3	1.4	1.9
Notropis buccatus	Catchment runoff	30.6	7.6
n = 1892	Mean annual streamflow	21.8	7.0
rtg = 0.869 (2.385)	Catchment area	19.5	47.7
	Catchment road crossings	8.4	1.2
	Catchment BFI	5.6	4.9
	Stream order	3.9	7.1
	Catchment open water	3.9	0.1
	Mean June precipitation	3.2	12.1
	Mean January precipitation	3.2	12.3
Luxilus chrysocephalus	Mean annual streamflow	42.4	38.0
n = 460	Mean January precipitation	24.3	31.9
rtg = 1.613 (5.018)	Catchment area	8.6	7.7
	Catchment wetness index	7.9	3.7
	Catchment organic matter	5.9	4.8
	Catchment BFI	4.6	9.7
	Catchment runoff	4.4	1.7
	Catchment elevation	1.9	2.6
Semotilus atromaculatus	Catchment area	48.9	68.9
n = 3146	Mean annual streamflow	31.8	13.0
rtg = 0.510 (1.665)	Catchment road crossings	7.0	1.1
	Mean June precipitation	5.0	6.0
	Catchment runoff	3.8	3.8
	Stream order	2.2	5.0
	Catchment elevation	1.3	2.3

Table 2 (continued)

Percidae			
Etheostoma blennioides	Catchment area	47.4	50.4
n = 2617	Mean annual streamflow	30.8	25.8
rtg = 0.597 (1.817)	Catchment elevation	11.1	16.3
	Catchment open water	3.2	0.1
	Catchment runoff	3.1	3.7
	Catchment road crossings	2.6	0.3
	Mean January precipitation	1.8	3.3
Etheostoma caeruleum	Catchment area	42.8	44.0
n = 2365	Mean annual streamflow	25.3	19.2
rtg = 0.625 (1.868)	Catchment elevation	16.9	21.4
	Mean January precipitation	5.4	7.2
	Catchment road crossings	4.9	0.2
	Catchment runoff	4.7	8.0

Table 3. Given as percentages, differences in the median MaxEnt raw score between the RCP 4.5 and RCP 8.5 climate scenarios, relative to the historical scenario. Values given for the Ohio River Basin (ORB) and within the MTR buffer (MTR). Calculated as: % change = [future median raw score – historical median raw score] ÷ historical median raw score x 100.

		RCP 4.5		RCP 8.5	
Species		**ORB**	**MTR**	**ORB**	**MTR**
Catostomidae					
	Catostomus commersonii	1	-1	30	46
	Hypentelium nigricans	1	-1	45	61
Cottidae					
	Cottus bairdii	2	-2	53	66
Cyprinidae					
	Campostoma anomalum	2	-3	64	88
	Notropis buccatus	-20	-33	-29	-31
	Luxilus chrysocephalus	75	-1	636	418
	Semotilus atromaculatus	1	-3	36	47
Percidae					
	Etheostoma blennioides	6	19	70	119
	Etheostoma caeruleum	13	29	81	154

FIGURES

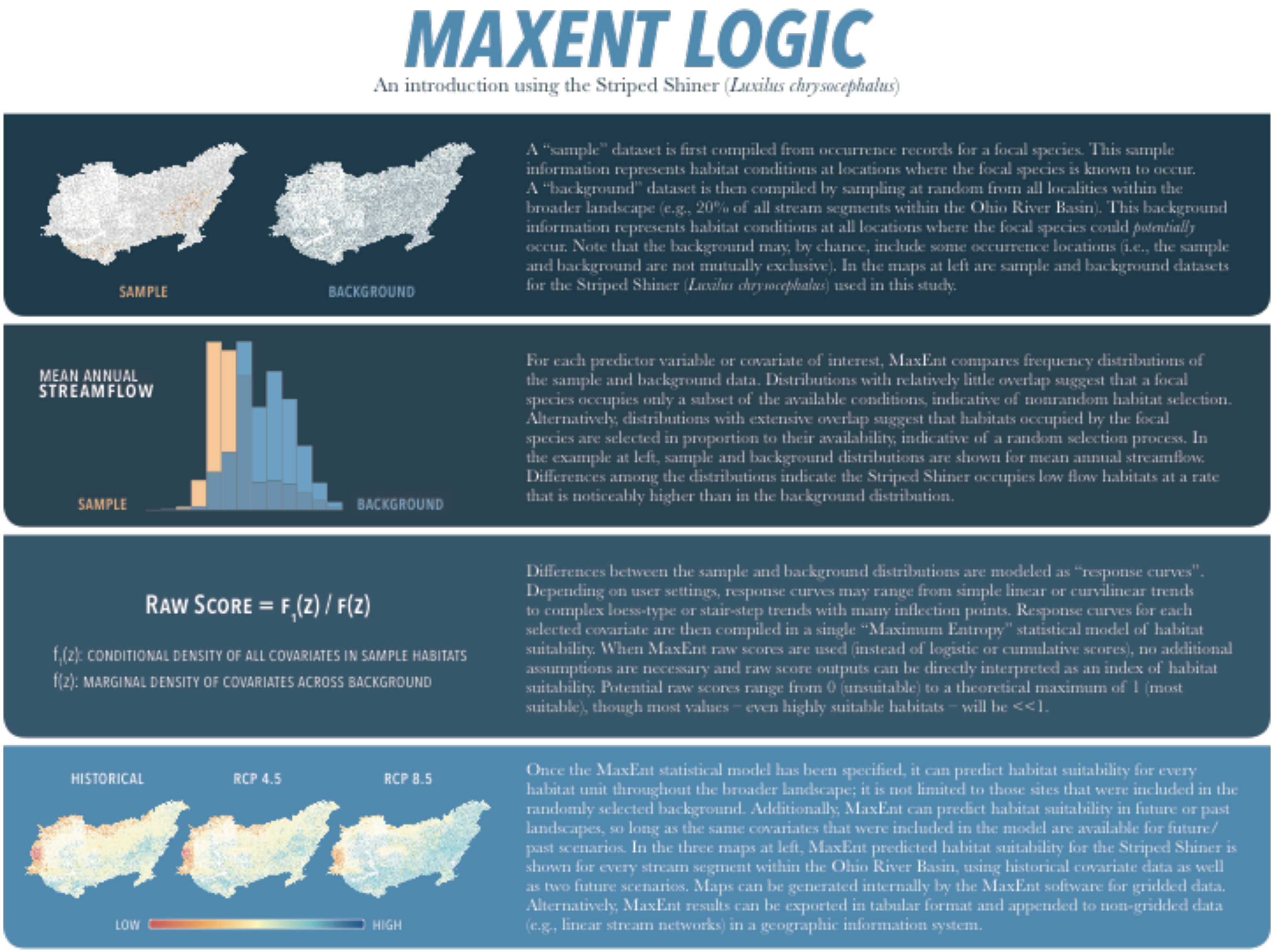

MAXENT LOGIC

An introduction using the Striped Shiner (*Luxilus chrysocephalus*)

A "sample" dataset is first compiled from occurrence records for a focal species. This sample information represents habitat conditions at locations where the focal species is known to occur. A "background" dataset is then compiled by sampling at random from all localities within the broader landscape (e.g., 20% of all stream segments within the Ohio River Basin). This background information represents habitat conditions at all locations where the focal species could *potentially* occur. Note that the background may, by chance, include some occurrence locations (i.e., the sample and background are not mutually exclusive). In the maps at left are sample and background datasets for the Striped Shiner (*Luxilus chrysocephalus*) used in this study.

For each predictor variable or covariate of interest, MaxEnt compares frequency distributions of the sample and background data. Distributions with relatively little overlap suggest that a focal species occupies only a subset of the available conditions, indicative of nonrandom habitat selection. Alternatively, distributions with extensive overlap suggest that habitats occupied by the focal species are selected in proportion to their availability, indicative of a random selection process. In the example at left, sample and background distributions are shown for mean annual streamflow. Differences among the distributions indicate the Striped Shiner occupies low flow habitats at a rate that is noticeably higher than in the background distribution.

RAW SCORE = $f_1(z) / f(z)$

$f_1(z)$: CONDITIONAL DENSITY OF ALL COVARIATES IN SAMPLE HABITATS

$f(z)$: MARGINAL DENSITY OF COVARIATES ACROSS BACKGROUND

Differences between the sample and background distributions are modeled as "response curves". Depending on user settings, response curves may range from simple linear or curvilinear trends to complex loess-type or stair-step trends with many inflection points. Response curves for each selected covariate are then compiled in a single "Maximum Entropy" statistical model of habitat suitability. When MaxEnt raw scores are used (instead of logistic or cumulative scores), no additional assumptions are necessary and raw score outputs can be directly interpreted as an index of habitat suitability. Potential raw scores range from 0 (unsuitable) to a theoretical maximum of 1 (most suitable), though most values – even highly suitable habitats – will be <<1.

Once the MaxEnt statistical model has been specified, it can predict habitat suitability for every habitat unit throughout the broader landscape; it is not limited to those sites that were included in the randomly selected background. Additionally, MaxEnt can predict habitat suitability in future or past landscapes, so long as the same covariates that were included in the model are available for future/past scenarios. In the three maps at left, MaxEnt predicted habitat suitability for the Striped Shiner is shown for every stream segment within the Ohio River Basin, using historical covariate data as well as two future scenarios. Maps can be generated internally by the MaxEnt software for gridded data. Alternatively, MaxEnt results can be exported in tabular format and appended to non-gridded data (e.g., linear stream networks) in a geographic information system.

Figure 1. A conceptual diagram of the MaxEnt species distribution modeling method, using data and results for the Striped Shiner.

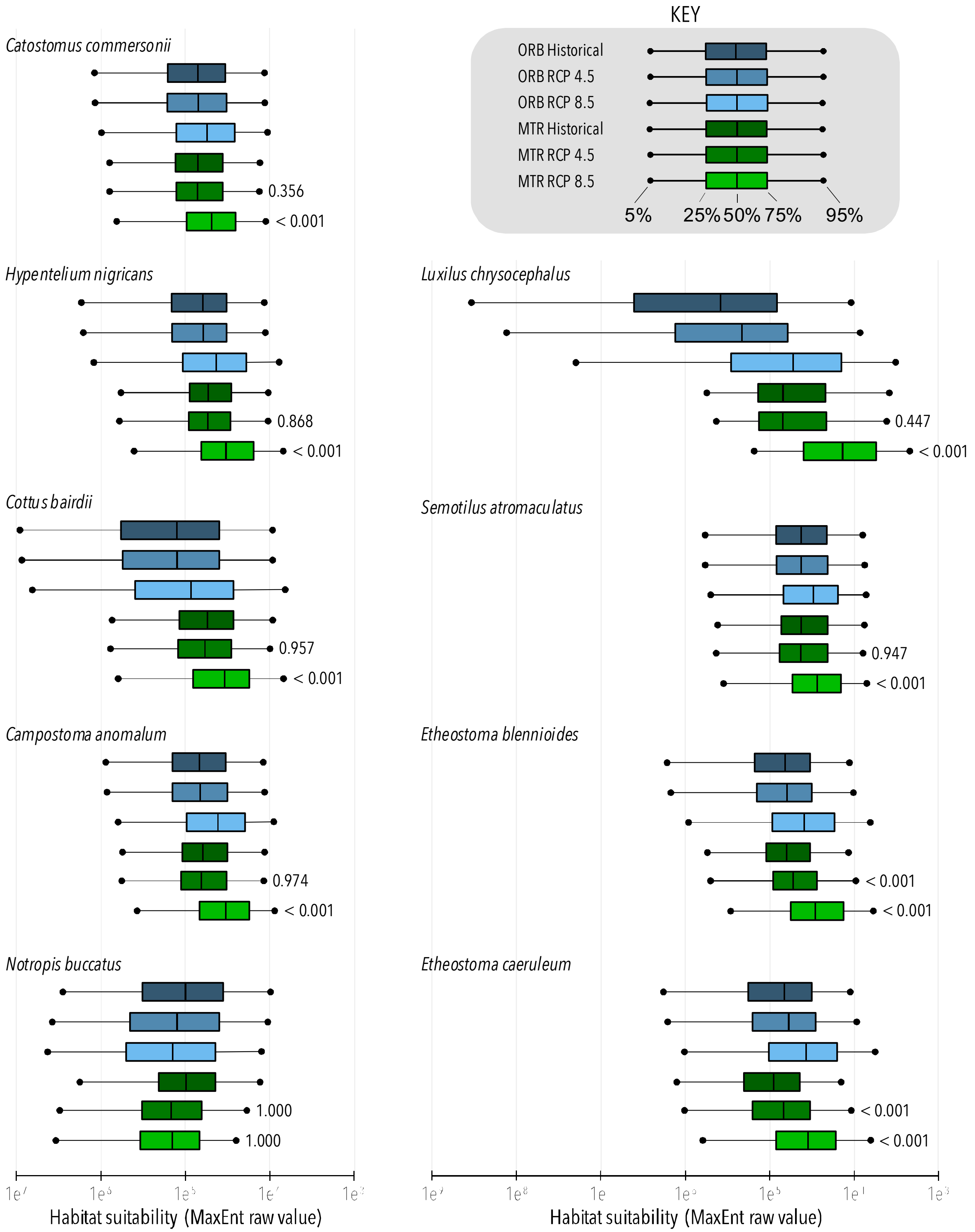KEY
ORB Historical
ORB RCP 4.5
ORB RCP 8.5
MTR Historical
MTR RCP 4.5
MTR RCP 8.5
5%
25%
50%
75%
95%
Catostomus commersonii
0.356
< 0.001
Hypentelium nigricans
0.868
< 0.001
Cottus bairdii
0.957
< 0.001
Campostoma anomalum
0.974
< 0.001
Notropis buccatus
1.000
1.000
Luxilus chrysocephalus
0.447
< 0.001
Semotilus atromaculatus
0.947
< 0.001
Etheostoma blennioides
< 0.001
< 0.001
Etheostoma caeruleum
< 0.001
< 0.001
1e/
1e6
1e5
1e/
1e3
Habitat suitability (MaxEnt raw value)
1e9
1e8
1e
1e6
1e5
1e1
1e3
Habitat suitability (MaxEnt raw value)

Figure 2. Boxplots of the distributions of MaxEnt raw scores. Box elements are standard percentiles (see key). For each species, the distributions of raw scores across the Ohio River Basin (ORB; blue boxes) and within the MTR buffer (MTR; green boxes) are shown for historical data as well as the RCP 4.5 and RCP 8.5 mid-century climate change scenarios. Mann-Whitney test *p*-values (paired sample tests using individual stream segments as replicates) comparing historical MaxEnt raw scores with future projections are shown for the RCP 4.5 and RCP 8.5 results within the MTR buffer.

Striped Shiner (*Luxilus chrysocephalus*)
mid-century habitat predictions

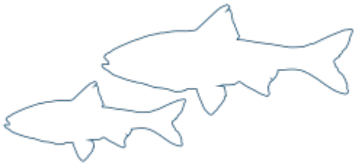

THREATS

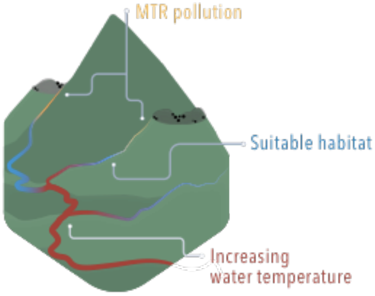

COVARIATES

Variables included in MaxEnt species distribution model; streamflow was the best predictor of presence

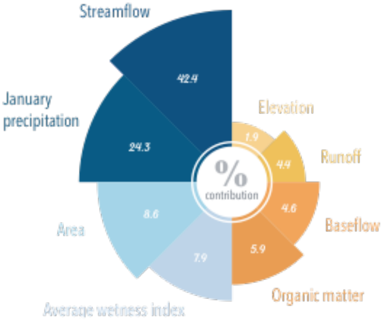

PREDICTED SUITABILITY

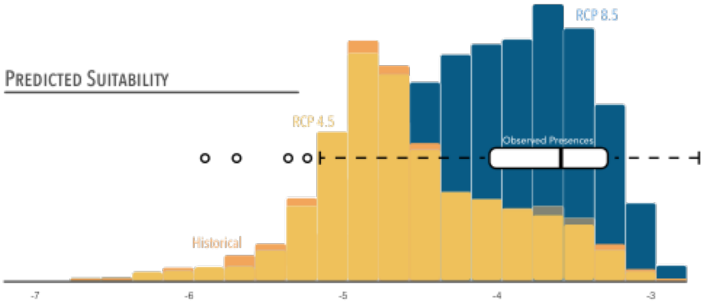

Distributions of MaxEnt raw scores within the MTR buffer, shown on a $\log_{10}$ scale, for historical and mid-century climate data. The historical and RCP 4.5 distributions are nearly identical, suggesting that Striped Shiner habitat will not change under RCP 4.5 conditions. However, habitat suitability may increase substantially under RCP 8.5. Note that the historically observed range of MaxEnt raw scores at sites of known occurrence (white box plot) closely matches the projected distribution of RCP 8.5 raw scores.

SHIFTS IN SUITABILITY

Within MTR buffer, percent change in suitability among future scenarios, relative to historical scenario

HABITAT SUITABILITY WITHIN MTR BUFFER

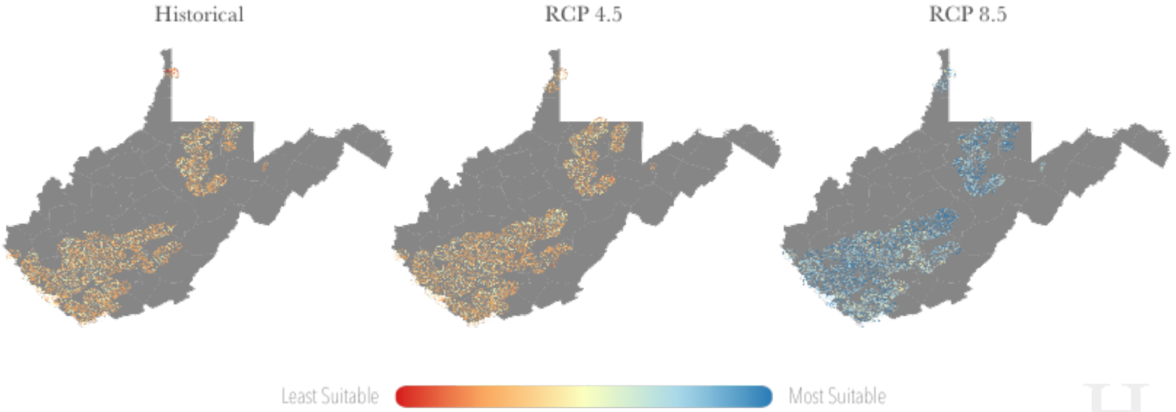

Figure 3. Infographic summary of MaxEnt modeling results for the Striped Shiner. Illustration at upper-left demonstrates the basic stream warming phenomenon that motivated this study. Plot at upper-right shows the percent contributions of the eight covariates that were retained in the final MaxEnt model. Histograms at center-left show distributions of MaxEnt raw scores ($\log_{10}$ scale) throughout the MTR buffer for historical model projections and the RCP 4.5 and RCP 8.5 future scenarios. A boxplot of calculated MaxEnt raw scores at sites of known presence is superimposed on the histograms. Bar chart at center-right shows the dramatic difference in predicted habitat suitability (i.e., average percent change in MaxEnt raw scores) among the RCP 4.5 and RCP 8.5 projections. Maps at bottom show the spatial distribution of stream segments within the MTR buffer that were predicted to have high and low habitat suitability values under historical and future conditions. A high-resolution copy of this infographic is available for download at https://doi.org/10.6084/m9.figshare.6089831.